UCSF

Title

An electroencephalographic signature predicts craving for methamphetamine.

Permalink

Journal

Authors

Tian, Weiwen
Zhao, Di
Ding, Jinjun
et al.

Publication Date

DOI

Article

An electroencephalographic signature predicts craving for methamphetamine

Graphical abstract
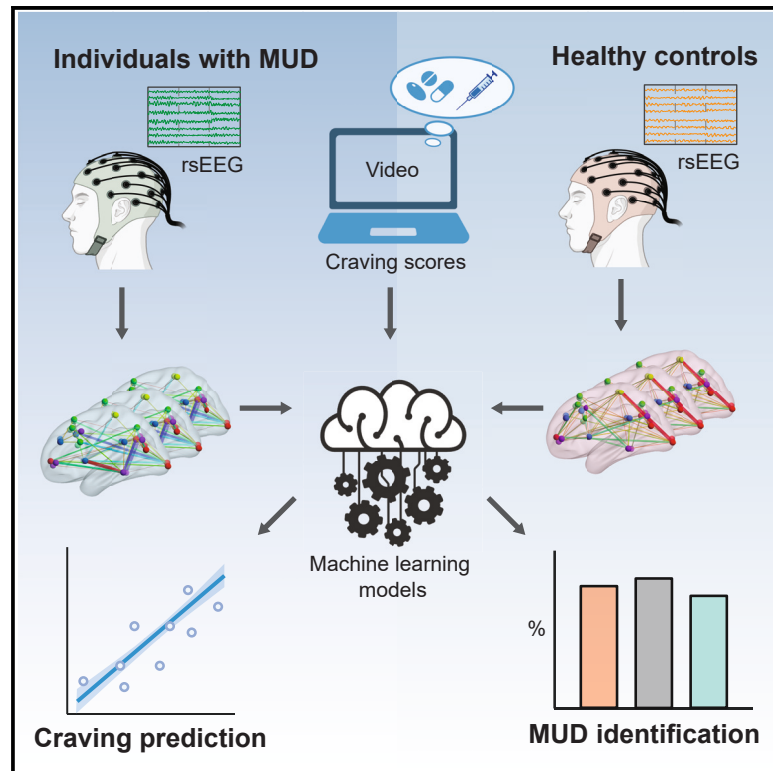
Authors

Weiwen Tian, Di Zhao, Jinjun Ding, ...,
Amit Etkin, Wei Wu, Ti-Fei Yuan

Correspondence

weiwuneuro@gmail.com (W.W.),
ytf0707@126.com (T.-F.Y.)

In brief

Tian et al. identify neurophysiological connectomic biomarkers for abnormality detection and craving prediction in individuals with methamphetamine use disorder (MUD) through machine learning (ML) models. The utilization of resting-state high-density electroencephalography (EEG) at the individual level presents a promising approach for clinical symptom evaluation, auxiliary diagnosis, and personalized treatment of MUD.

Highlights

- We identify an individual-level neurobiological connectomic craving signature for MUD

- Resting-state high-density EEG offers clinically feasible, translatable MUD biomarker

- ML models at individualized level help to explain individual variability in MUD

CellPress

Cell Reports Medicine

Article

An electroencephalographic signature predicts craving for methamphetamine

Weiwen Tian,[1,7] Di Zhao,[1,7] Jinjun Ding,[1] Shulu Zhan,[1] Yi Zhang,[1] Amit Etkin,[2,3,4] Wei Wu,[2,3,4,*] and Ti-Fei Yuan[1,5,6,8,*]

[1]Shanghai Key Laboratory of Psychotic Disorders, Brain Health Institute, National Center for Mental Disorders, Shanghai Mental Health Center, Shanghai Jiaotong University School of Medicine, Shanghai 200030, China
[2]Department of Psychiatry and Behavioral Science, Stanford University, Stanford, CA 94305, USA
[3]Wu Tsai Neuroscience Institute, Stanford University, Stanford, CA 94305, USA
[4]Alto Neuroscience, Inc., Los Altos, CA 94022, USA
[5]Institute of Mental Health and Drug Discovery, Oujiang Laboratory (Zhejiang Lab for Regenerative Medicine, Vision and Brain Health), Wenzhou, Zhejiang 325000, China
[6]Co-innovation Center of Neuroregeneration, Nantong University, Nantong, Jiangsu 226019, China
[7]These authors contributed equally
[8]Lead contact
*Correspondence: weiwuneuro@gmail.com (W.W.), ytf0707@126.com (T.-F.Y.)
https://doi.org/10.1016/j.xcrm.2023.101347

SUMMARY

Craving is central to methamphetamine use disorder (MUD) and both characterizes the disease and predicts relapse. However, there is currently a lack of robust and reliable biomarkers for monitoring craving and diagnosing MUD. Here, we seek to identify a neurobiological signature of craving based on individual-level functional connectivity pattern differences between healthy control and MUD subjects. We train high-density electroencephalography (EEG)-based models using data recorded during the resting state and then calculate imaginary coherence features between the band-limited time series across different brain regions of interest. Our prediction model demonstrates that eyes-open beta functional connectivity networks have significant predictive value for craving at the individual level and can also identify individuals with MUD. These findings advance the neurobiological understanding of craving through an EEG-tailored computational model of the brain connectome. Dissecting neurophysiological features provides a clinical avenue for personalized treatment of MUD.
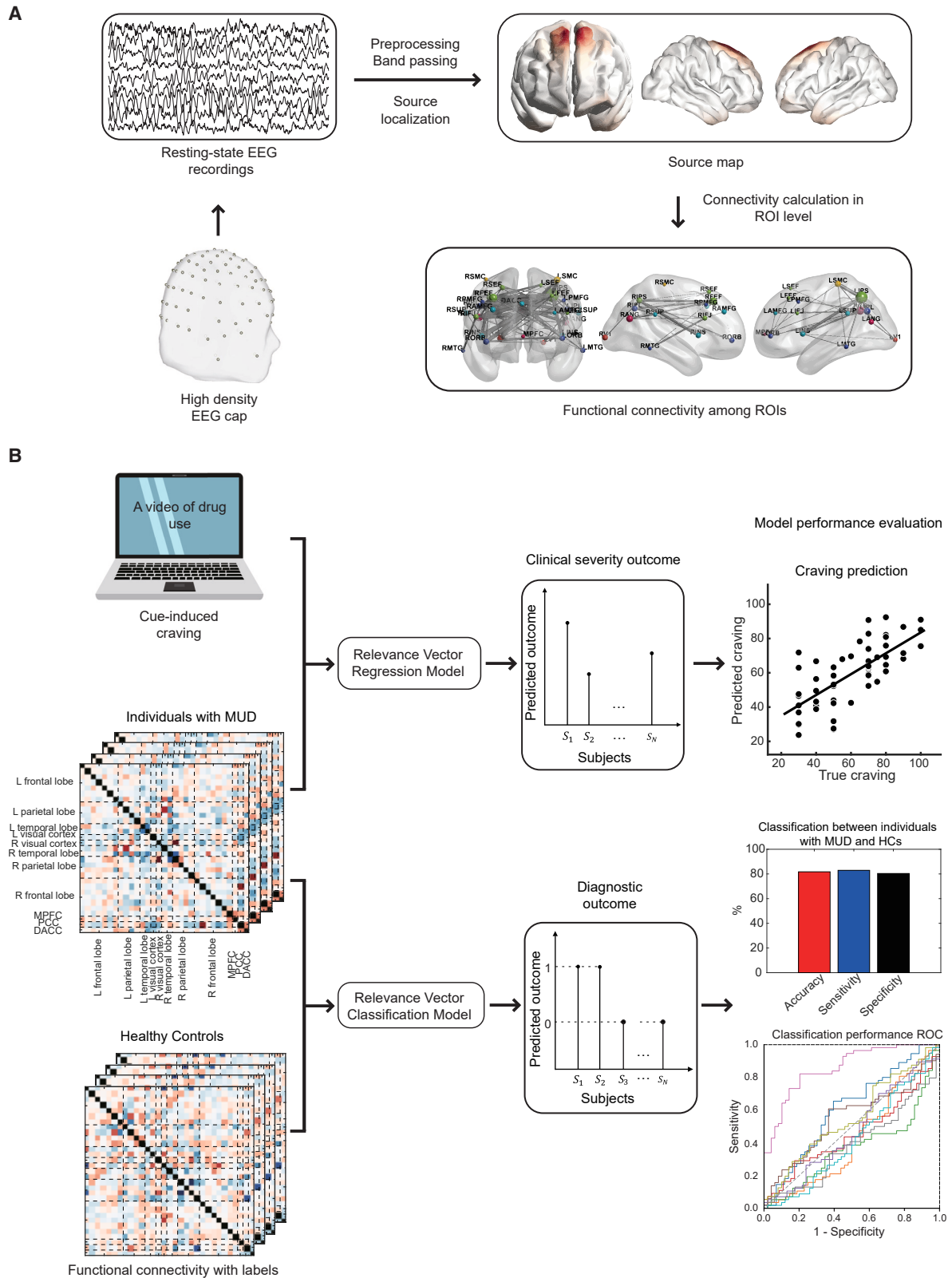
INTRODUCTION

Methamphetamine use disorder (MUD) is a prevalent substance use disorder (SUD) with a high relapse rate.[1] According to the 2020 National Survey on Drug Use and Health, the methamphetamine use prevalence of individuals aged 12 or older increased by over 50% from 2017 to 2020.[2] The consequences of methamphetamine use and addiction result in a significant cost. However, current interventions for MUD have limited efficacy, with a high relapse rate of about 61%.[3] Moreover, there is significant heterogeneity among clinical MUD syndromes.[4] Identifying reliable biomarkers of methamphetamine use and relapse is crucial to assisting with diagnosis, monitoring, prognosis, and treatment by tailoring interventions more effectively to each individual with MUD.

Craving and drug cue reactivity are considered central mechanisms and critical predictors of drug use outcome and relapse.[5,6] They are included in DSM-5 as a diagnostic criterion for SUD.[7] Cue-elicited craving serves as a good predicator of subsequent drug use and relapse in the clinical population,[5,8] while treatments targeting craving can reduce drug use and prevent relapse.[5,9] A recent systematic review and meta-analysis emphasized that craving is one of the most important clinical indicators across all stages of treatment, including primary clinical care.[10] There has been a continuing need to investigate the neurobiological bases underlying craving and MUD.

Compared to neuroimaging approaches such as functional magnetic resonance imaging (fMRI) and positron emission tomography (PET), scalp electroencephalography (EEG) has the advantage of high temporal resolution, low cost, and easy data acquisition, offering a viable path for translating biomarkers of craving in subjects with SUD. However, conventional 32- or 64-channel scalp EEGs perform poorly in source localization analysis, as the effect of volume conduction can substantially change the scalp EEG signal.[11] Notably, the use of high-density EEG (128 channels or higher) could largely alleviate the effects of volume conduction.[12] A high-density EEG system provides direct assessments of regional and global activity, through which brain activities can be reconstructed by applying precise source imaging.[13] Traditional resting EEG biomarkers of abnormal brain activities have proven useful in the assessment of epilepsy[14] and have also demonstrated promise for depression, both for diagnosis and treatment prediction.[15,16] Identifying EEG signatures of craving may yield mechanistic insight into craving, provide

A

Resting-state EEG recordings

Preprocessing
Band passing

Source localization

Source map

High density EEG cap

Connectivity calculation in ROI level

Functional connectivity among ROIs

B

A video of drug use

Cue-induced craving

Individuals with MUD

L frontal lobe
L parietal lobe
L temporal lobe
L visual cortex
R visual cortex
R temporal lobe
R parietal lobe
R frontal lobe
MPFC
PCC
DACC

Relevance Vector Regression Model

Clinical severity outcome

Model performance evaluation

Craving prediction

Relevance Vector Classification Model

Diagnostic outcome

Classification between individuals with MUD and HCs

Classification performance ROC

Healthy Controls

Functional connectivity with labels

(legend on next page)

novel brain targets, and offer feedback signals for developing closed-loop neurostimulation therapies for MUDs.

To understand the neurophysiological architecture of MUD, researchers have typically used two approaches. The first approach is hypothesis driven, where researchers compare different groups (e.g., a group of individuals with MUD and a control group) to probe the clinical relevance of specific neural signals in line with the *a priori* hypotheses. For example, previous studies have suggested that increased slow-wave activity (delta and theta) in methamphetamine abusers and increased beta band synchronization of the medial prefrontal cortex (MPFC) are associated with enhanced cued craving.[17,18] In this approach, previous EEG evidence is used to determine the neural indicators that will be measured, which population will be tested, and which analytical method will be carried out. Using such an approach, although multiple brain regions have been identified as relevant to craving in MUD and capable of distinguishing between healthy control individuals and patients with MUD, these associations and statistically significant distinctions have not yielded a robust biomarker for individuals with MUD. The hypothesis-driven approach seeks to elucidate the variance or disparities between multiple variables but has limited applicability to novel individuals.

The second approach employs data-driven machine learning methods, which use a variety of neurobiological features for MUD classification and craving prediction. For instance, Ding et al. proposed using the mean and standard deviation (SD) of absolute EEG power and galvanic skin response to classify individuals with MUD and healthy control individuals, achieving an accuracy of 90.68%.[19] Li et al. used arterial spin labeling to classify individuals with MUD and healthy control individuals, covering related brain circuits including the occipital lobe, insular cortex, postcentral gyrus, corpus callosum, and inferior frontal cortex.[20] These studies have shown promising results in classification, but the low-density EEG poses challenges in effectively modeling features of input connections topology. The neural substrate underlying cued craving is inconsistent and variable at the individual level. As of yet, biomarkers have not been successfully used to predict cravings and identify individuals with MUD at the individual level in a reliable manner. Here, data-driven machine learning methods can potentially harness discriminating information within the data more effectively, and the resulting models can be assessed for overfitting through validation on independent samples.

Here, leveraging high-density 128-channel resting-state EEG, we sought to investigate the neurophysiological connectomes of MUD and identify biomarkers for identification of abnormality and craving at the individual level. Our study builds upon previous EEG studies of MUD as follows: (1) a total of 153 subjects (101 in-dividuals with MUD and 52 well-matched healthy control [HC] individuals) were included in the study to increase statistical power compared to previous studies with smaller samples. (2) We estimated brain functional connectivity networks (FCNs) from resting-state EEG in individuals with MUD and HC individuals, both for group comparison and as features for machine learning models (Figures 1A and 1B). The FCNs were quantified using imaginary coherence (iCoh), which is defined as the imaginary part of coherency and not confounded by volume conduction.[21] (3) The use of high-density EEG and iCoh functional connectivity allowed us to identify a robust neurobiological biomarker for MUD brain abnormalities and correlates of craving. (4) Our machine learning analysis of neurobiological biomarkers at the individual level helped to explain individual variability and suggest more efficient measures to be used to develop artificial intelligence (AI) methodologies in supporting diagnosis of MUD. Our aim in this study was to identify a transdiagnostic, reliable neurobiological biomarker by utilizing machine learning models on individual-level functional connectivity data in order to classify individuals with MUD and predict craving in those individuals.

RESULTS

Group-level analysis with EEG FCNs

EEG FCNs for 57 individuals with MUD and 52 HC individuals (Table 1; Figure S1) were computed. EEG FCNs were calculated between 465 region of interest (ROI) pairs (among 31 ROIs) across 5 carrier frequency bands (delta, theta, alpha, beta, and gamma) with 2 resting conditions (resting-state eyes closed and resting-state eyes open) from cortical current source density in source space (see STAR Methods). Pearson's r values were used to quantify the correlations between FCNs and craving scores in individuals with MUD (Figures 2A and 2B). The results indicated significant correlations between craving and LINS (left insula)-RORB (right orbital gyrus) connections in the delta frequency band in the resting-state eyes open (REO) condition (hereafter referred to as REO delta; $r = 0.505$, $p = 0.029$, false discovery rate [FDR] corrected), as well as LPMFG (left posterior middle frontal gyrus)-MPFC connections in REO beta ($r = 0.500$, $p = 0.034$, FDR corrected) and RSUP (right supramarginal gyrus)-PCC (posterior cingulate cortex) connections in REO beta ($r = 0.473$, $p = 0.047$, FDR corrected). No significant correlations were found with other connections in REO delta or REO beta. No significant correlations were found in resting-state eyes-closed conditions or in other frequency bands in REO conditions.

Furthermore, we conducted an independent-sample t test on EEG FCNs across 465 ROI pairs to determine whether they could differentiate individuals with MUD from HC individuals. Our results revealed a significant difference between the two groups

---

Figure 1. MUD biomarker identification framework

(A) EEG processing and functional connectivity feature extraction. EEG data were collected using a high-density EEG cap. After EEG preprocessing and band passing, we conducted source localization using sensor-level data and obtained cortical current source density in source space. Then functional connectivity (iCoh) was extracted at the ROI level.

(B) Individual-level analysis pipeline. FCNs in individuals with MUD were used to predict craving with relevance vector machine model. Relevance vector machine model was also applied in the abnormality identification between individuals with MUD and HC individuals. For craving score prediction, Pearson's correlation coefficient and root-mean-square errors (RMSEs) were calculated to evaluate the performance. For MUD vs. HC classification, accuracy, sensitivity, specificity, and ROC curve were calculated.

Table 1. Demographic and clinical characteristics of individuals with MUD and healthy control individuals

Demographic information on individuals with MUD and healthy control individuals

Variable	MUD dataset 1	MUD dataset 2	Healthy control individuals	F	t	p
n	57	44	52	–	–	–
Age	34.8 years (7.2)	34.8 years (7.6)	36.6 years (10.0)	0.743	–	0.477
Educational attainment	8.8 years (3.6)	9.3 years (2.0)	9.2 years (2.5)	0.496	–	0.610
First age of use/addiction	26.1 years (6.4)	26.1 years (7.0)	–	–	−0.049	0.961
Addiction years	7.9 years (4.3)	8.1 years (4.5)	–	–	−0.230	0.819
Usage per month before abstinence	17.1 g/month (15.7)	15.6 g/month (10.7)	–	–	0.537	0.592
Duration of current abstinence before experiment	10.3 months (8.5)	6.6 months (6.6)	–	–	2.337	0.021
Number of DSM-V symptoms	7.9 (1.7)	8.1 (1.9)	–	–	−0.565	0.574
Craving scores	60.4 (21.1)	60.7 (22.6)	–	–	−0.075	0.940

57 individuals with MUD in MUD dataset 1, 44 individuals with MUD in MUD dataset 2, and 52 HC individuals were included in the analysis. Values are presented as mean with standard deviation in parentheses. One-way ANOVA was conducted to compare age and educational attainment in MUD dataset 1, MUD dataset 2, and HC individuals. Independent t test was conducted to compare first age of use/addiction, methamphetamine usage per month before abstinence, duration of current abstinence before experiment, number of DSM-V symptoms, and craving scores in MUD dataset 1 and MUD dataset 2.

in the strength of connections between LSMC (left somatosensory cortex) and LV1 (left visual area 1) ($t = -4.188$, p = 0.027, FDR corrected) and in connections between RINS (right insula) and RSEF (right supplementary eye fields) ($t = 3.986$, p = 0.029, FDR corrected) in REO beta (Figures 2C and 2D). No significant differences were found in other connections in REO beta. No significant differences were found in other frequency bands.

In addition to the relationship between neurobiological measurements and craving, we also calculated correlations between craving and behavioral measurements, including the Pittsburgh Sleep Quality Index (PSQI), the Beck Depression Inventory (BDI-II), Barratt Impulsivity Scale (BIS-II) subscores (attention, motor, no plan, and total impulsiveness), and Barratt Anxiety Inventory (BAI). However, none of these behavioral variables showed a significant correlation with craving scores.

EEG connectomic biomarker for craving prediction at the individual level

We next investigated whether EEG FCNs could serve as biomarkers for MUD craving (measured as peak-provoked craving [PPC]) at the individual level. To accomplish this, we used a relevance vector machine (RVM) to build models that predicted craving scores in individuals with MUD (MUD dataset 1) (STAR Methods; Figures S2A and S2B). The predictive performance of models built for all frequency bands and resting conditions is shown in Figure S3. The models based on REO beta and REO delta were able to significantly predict the craving scores (Figures 3A–3C). Specifically, the REO delta model showed a Pearson's r of 0.41, p = 0.009 (FDR corrected), with a root-mean-square error (RMSE) of 21.60, while the REO beta model exhibited a highest performance with Pearson's r = 0.73, p < 3×10^{-9} (FDR corrected), and RMSE = 14.75.

To assess the importance of EEG FCNs in predicting individual craving scores using RVM models for REO delta and REO beta, we evaluated the weights of the connections in the models

(Figures 3D–3G). As the RVM model is a sparse model, only a few connections contribute to the model and are important for the prediction. In the REO delta model, important connections included those among RORB and LMTG (left middle temporal gyrus) in the frontoparietal control network, INS (insula) and SUP (supramarginal gyrus) in the ventral attention network, and FEF (frontal eye fields) in the dorsal attention network (e.g., RORB-LINS, LSMC-RSUP, LIPS [left intraparietal sulcus]-RINS, LMTG-LSUP [left supramarginal gyrus], LMTG-LIFJ [left inferior frontal junction], RFEF [right frontal eye fields]-RANG [right angular gyrus], and LFEF [left frontal eye fields]-LPMFG). In contrast, the REO beta model was predominantly driven by connections between the MPFC and LPMFG, as well as connections between PCC and RSUP, which were also significantly correlated with craving scores in the univariate group-level analysis (Figure 2B). Additionally, connections with RAMFG (right anterior midlle frontal gyrus) in the ventral attention network (LSEF (left supplementary eye fields)-RAMFG and LIPL (left inferior parietal lobule)-RAMFG) were also important for prediction. A more detailed list of the important connections in the REO delta and REO beta models is provided in Table S1.

Despite the weak correlations observed between the craving scores and behavioral measurements in the univariate analysis, it was still possible that combining behavioral measurements with EEG features could enhance the predictive performance. However, this was not found to be the case. Combining EEG connectivity features with behavioral measurements did not lead to an improvement in the performance of the model in predicting craving scores.

Replication of craving prediction in the other independent MUD dataset

We tested whether our craving prediction models could be replicated by conducting the same analysis on an independent resting-state EEG dataset of 44 individuals with MUD (MUD
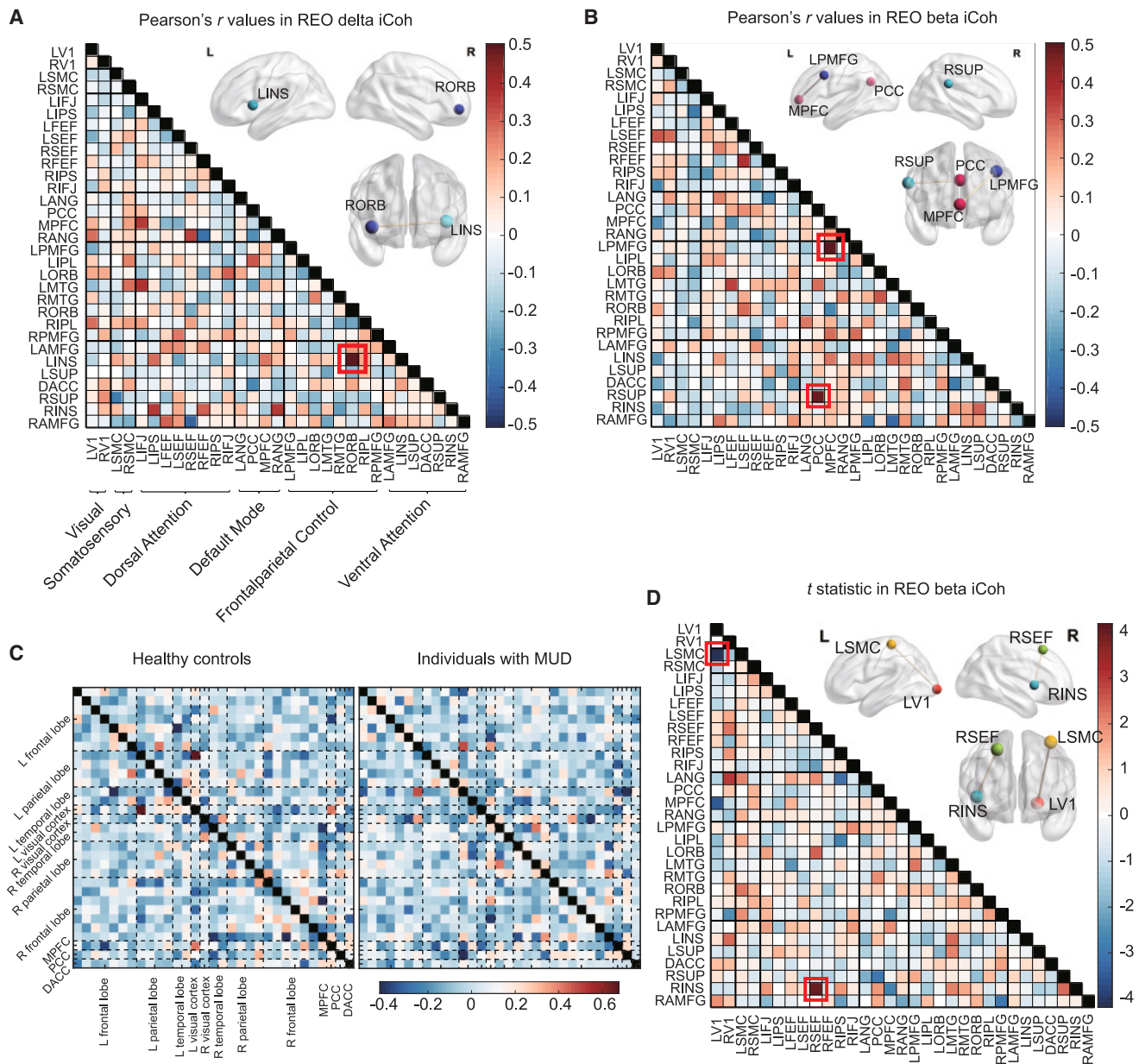
Figure 2. Resting-state EEG iCoh connectomes in the discovery MUD dataset and HC dataset

(A) Pearson's r values in REO delta iCoh between FCNs and craving scores in individuals with MUD (n = 57 individuals with MUD). Only the correlations between LINS and RORB (r = 0.505, p = 0.029, FDR corrected) survived correction for multiple comparisons. Inset: the connections between LINS and RORB in brain networks.

(B) Pearson's r values in REO beta iCoh between FCNs and craving (n = 57 individuals with MUD). The correlations between LPMFG and MPFC (r = 0.500, p = 0.034, FDR corrected) and the correlations between RSUP and PCC (r = 0.473, p = 0.047, FDR corrected) survived correction for multiple comparisons. Inset: LPMFG-MPFC connections and RSUP-PCC connections in brain networks.

(C) Mean REO beta connectivity matrices of all individuals with MUD and HC individuals (n = 57 individuals with MUD and 52 HC individuals). ROIs were divided into frontal lobe, parietal lobe, temporal lobe, visual cortex, MPFC, PCC, and DACC.

(D) t statistic in REO beta iCoh between individuals with MUD and HC individuals (n = 57 individuals with MUD and 52 HC individuals). The differences of the connections between LSMC and LV1 (t = −4.189, p = 0.027, FDR corrected) and the connections between RINS and RSEF (t = 3.986, p = 0.029, FDR corrected) were significant. Inset: LSMC-LV1 connections and RINS-RSEF connections in brain networks.

dataset 2). First, we tested the model performance of REO beta, the best predictor trained on dataset 1, using dataset 2 (Figure S4A). We observed a relatively high level of performance (Pearson's r = 0.60, p < 2 × 10⁻⁵, RMSE = 19.31), which was only slightly lower than the performance on the training dataset (dataset 1; Figure 3B). This result demonstrates the robustness
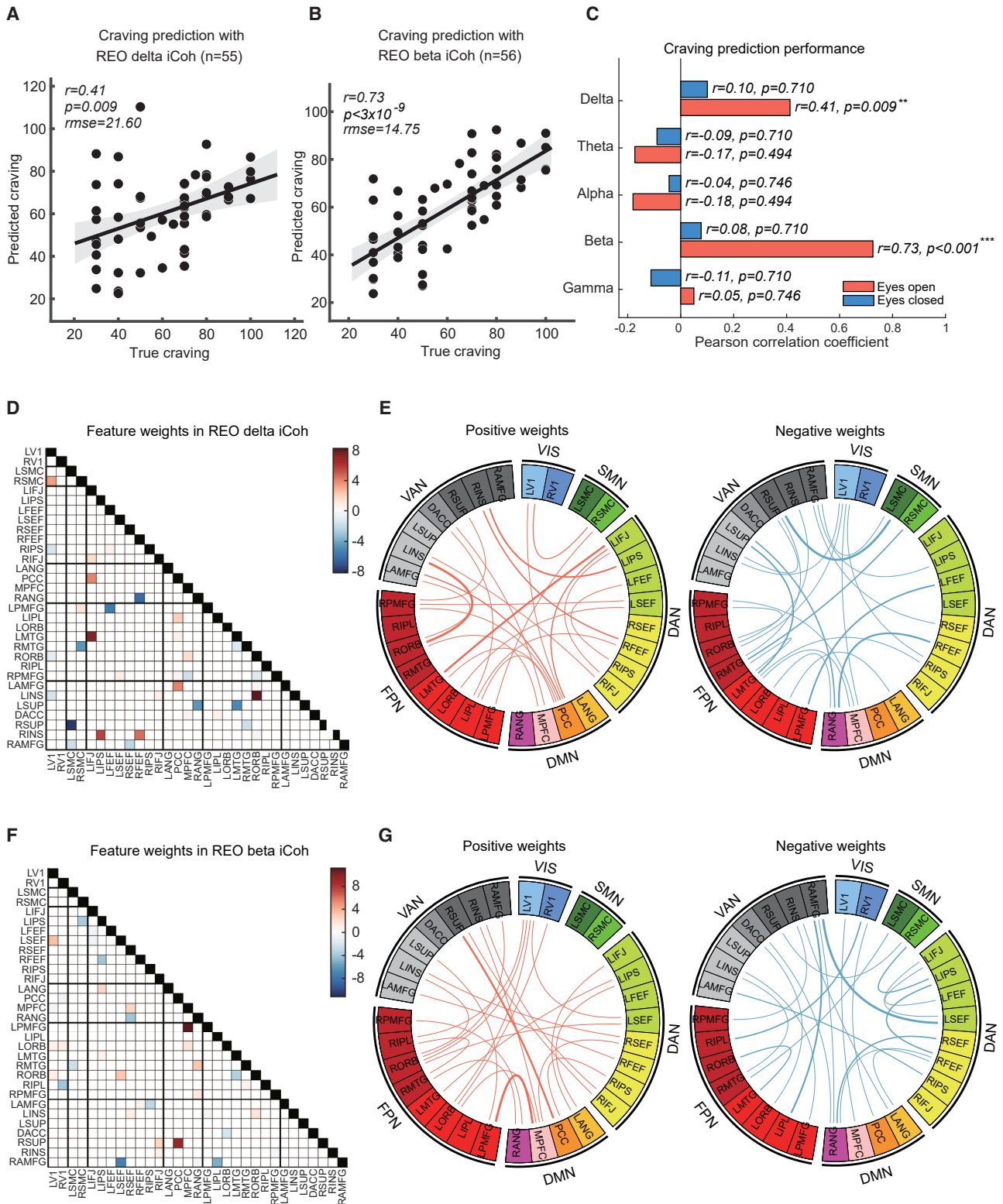
Figure 3. Resting-state EEG iCoh connectomes predict craving in individuals with MUD in dataset 1

(A) Predictive performance of REO delta iCoh model: Pearson's *r* = 0.41, p = 0.009, FDR corrected, RMSE = 21.60 (n = 55 individuals with MUD). Gray: 95% confidence interval.

of the craving prediction model trained on REO beta from dataset 1.

Next, we used MUD dataset 2 as an independent dataset and conducted 10-time 10-fold cross-validation. The prediction performance of models built for all frequency bands and resting conditions is shown in Figure S5. The REO beta model was able to significantly predict the craving scores (Figures S4B and S4C; Pearson's $r = 0.65$, $p < 2 \times 10^{-5}$, FDR corrected, RMSE = 17.56), consistent with the results from the discovery MUD dataset. However, compared to dataset 1, the REO delta model did not show significant prediction (Figures S4C and S5; Pearson's $r = 0.29$, $p = 0.222$, FDR corrected, RMSE = 22.78). In line with the results obtained from the discovery dataset, the results from the REO beta model trained on MUD dataset 2 demonstrate the robustness of our RVM model in predicting craving in individuals with MUD.

We then evaluated the weights of the RVM models for REO beta trained on dataset 2 (Figures S4D and S4E). As with the weights trained on dataset 1, the connections within and among MPFC, RSUP, and AMFG (anterior middle frontal gyrus) (e.g., MPFC-RANG and RSUP-LAMFG (left anterior middle frontal gyrus)) were observed to play an important role in the prediction. In addition, connections between RSEF and LANG (left angular gyrus) were also important to the prediction.

EEG connectomic biomarker for the identification of individuals with MUD

We proceeded to investigate whether EEG FCNs could serve as biomarkers for identifying MUD at the individual level. We employed the RVM model to classify individuals with MUD and HC individuals using FCNs from each frequency band and resting condition (STAR Methods). The predictive performance of the RVM classification models was evaluated with 10-time 10-fold cross-validation, presented in Figures 4 and S6. Consistent with the group-level results, the REO beta model demonstrated the best classification performance across all frequency bands and resting conditions, achieving a classification accuracy of 80.95% (sensitivity: 82.14%; specificity: 79.59%), which was substantially higher than that of the other models (all with classification accuracies below 70%; Figure S6). Furthermore, the REO beta model also exhibited the highest area under the operating characteristic curve (AUC; 0.859, Figure 4B) and diagnostic odds ratio (DOR; 17.94; Figure 4C) compared to other frequency bands and resting conditions.

To determine the contribution of different connections to the identification of individuals with MUD, we evaluated and visualized the weights of the REO beta RVM classification model, as shown in Figures 4D and 4E. Based on the feature weights, con-

nections among the primary visual cortex and insula were important for the classification, such as LINS-RV1 (right visual area 1), RINS-RSEF, and LV1-LSMC. Notably, the RINS-RSEF and LV1-LSMC connections were also found to differ significantly between the MUD and HC groups (Figure 2D). More details about important connections in the REO beta model can be found in Table S2.

Machine learning analysis using sensor-space spectral power features

Besides FCNs, EEG spectral powers are also used as alternative features to characterize oscillatory activities in the brain. However, it remains unclear whether the band power spectrum can truly reflect the alterations in brain function and the neural mechanisms underlying neurological and psychiatric disorders. Furthermore, it is unknown whether FCNs encode more information about MUD. To address these questions, we developed machine learning models based on spectral powers in sensor space to assess the ability of band powers to generate EEG biomarkers for individuals with MUD. We applied similar RVM models with sensor-space band powers as the input features for craving prediction and identification of MUD (STAR Methods).

The predictive performance of the resulting models was significantly inferior to that of the source-space connectivity-based models (Figure 5). The prediction performance of band power models built for all frequency bands and resting conditions is shown in Figure S7. Specifically, for craving score prediction, only the REO alpha power feature yielded a significantly predictive model (Figures 5A–5C; Pearson's $r = 0.47$, $p = 0.003$, FDR corrected, RMSE = 22.66), which was still considerably worse than REO beta iCoh. Concerning the classification of individuals with MUD and HC individuals, the best classification accuracy achieved was 64.22% using resting-state eyes closed (REC) gamma power features (Figures 5D–5F), which was much lower than the FCN models with 80.95% accuracy utilizing the source-space REO beta iCoh features. REO beta power feature had weak performance both in prediction (Figures 5A and S7; Pearson's $r = 0.10$, $p = 0.700$, FDR corrected, RMSE = 30.00) and classification (Figures 5D, 5E, and S7; accuracy = 60.55%, sensitivity = 63.16%, specificity = 57.69%, AUC = 0.604, DOR = 2.34) compared to REO beta iCoh performance (Figures 3B, 3C, 4A–4C, S3, and S6).

DISCUSSION

The current study employed a two-pronged approach, combining (1) theoretical analysis to compare the connectomic profiles of healthy individuals to those with MUD and (2) a

---

(B) Predictive performance of REO beta iCoh model: Pearson's $r = 0.73$, $p < 3 \times 10^{-9}$, FDR corrected, RMSE = 14.75 (n = 56 individuals with MUD). Gary: 95% confidence interval.

(C) Predictive performance comparisons between different predictors. Pearson's correlation, **$p < 0.01$; ***$p < 0.001$.

(D) Feature weight matrix for REO delta iCoh model.

(E) Connections of REO delta iCoh that contributed to the prediction with positive and negative weights, respectively. VIS: visual network; SMN: somatosensory network; DAN: dorsal attention network; DMN: default mode network; FPN: frontoparietal control network; VAN: ventral attention network.

(F) Feature weight matrix for REO beta iCoh model.

(G) Connections of REO beta iCoh that contributed to the prediction with positive and negative weights, respectively.

See also Figures S3–S5 and Table S1.
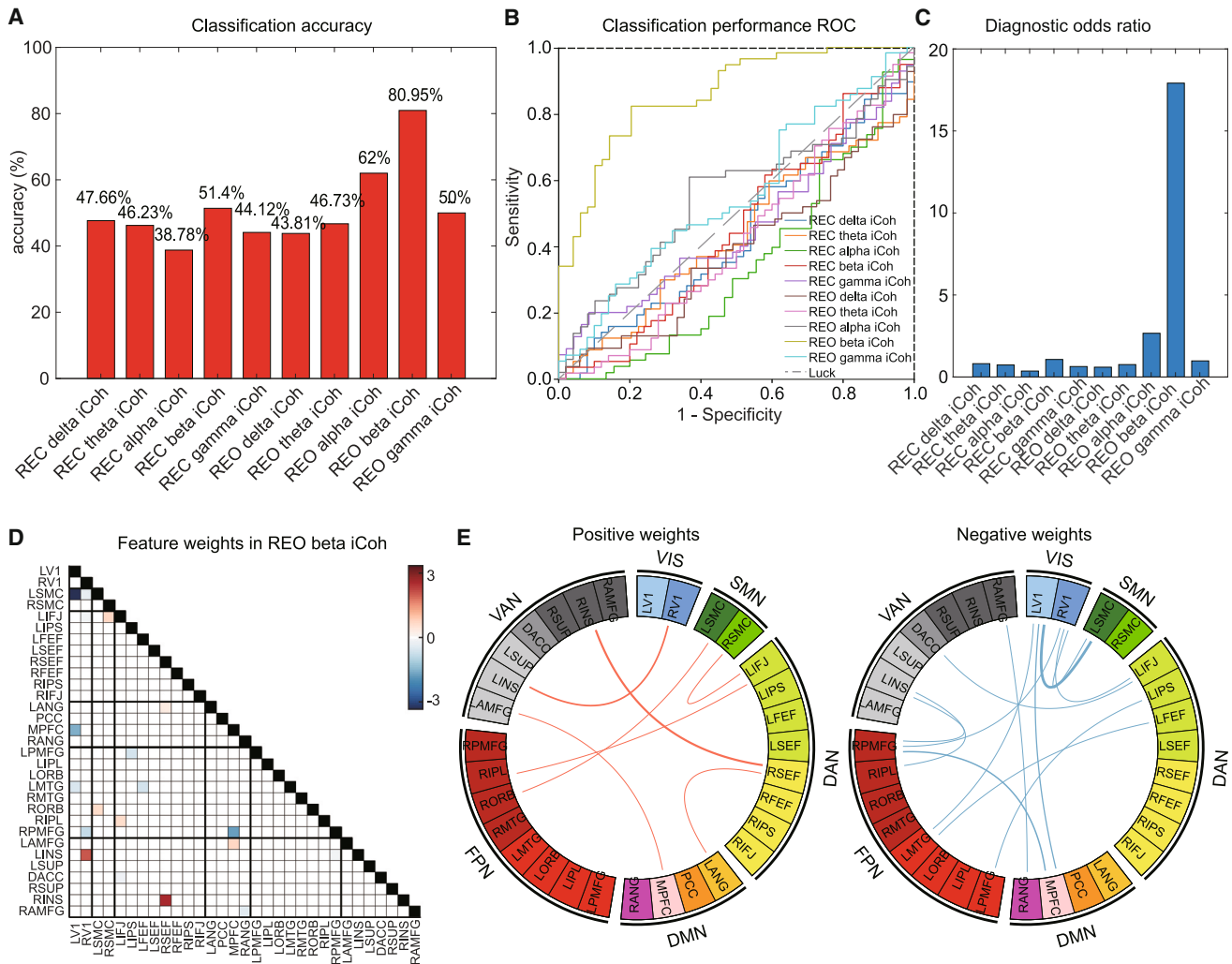
Figure 4. Identification of individuals with MUD by EEG iCoh connectomes

(A) Accuracy of classification performance of different carrier bands.

(B) Receiver operating characteristic curve (ROC) of classification performance.

(C) Diagnostic odds ratio of classification performance.

(D) Feature weight matrix for REO beta iCoh model.

(E) Connections that contributed to the identification of individuals with MUD. Red edges: positive weights; blue edges: negative weights. Edges are thicker for connections with a larger contribution.

See also Figure S6 and Table S2.

machine learning approach to identify neurobiological bio-markers for craving evaluation and MUD identification based on high-density EEG functional connectivity during resting-state recording. Unlike current EEG biomarkers for diagnosing brain diseases, this method utilized EEG source imaging to explore the complex interaction between brain regions and contrasted the results with the sensor-based dynamics of MUD. Our findings revealed nodes and network connectivity patterns that could serve as potential brain circuit markers for developing more targeted, mechanism-based therapeutics for MUD. With a precise connectomic road map, our findings lay the groundwork for machine-learning-driven personalized neuromodulation interventions and psycho-therapeutics for individuals with MUD.

Across our identified machine learning models, predictive brain regions such as the MPFC, angular gyrus, orbital gyrus, and insula, as well as their connections, were investigated in detail for craving prediction and MUD identification, consistent with previous studies of MUD.[18,22,23] In our previous studies, we demonstrated increased synchronization of the MPFC in the beta frequency band in individuals with MUD who had abstained from substance use for 1–3 months, which correlated with the incubation of craving.[18] The connections between the orbitofrontal cortex and other brain regions were found to be weaker in individuals with MUD compared to HC individuals in another study.[23] Moreover, individuals with MUD exhibit gray-matter volume deficits in the orbitofrontal cortex, angular gyrus,
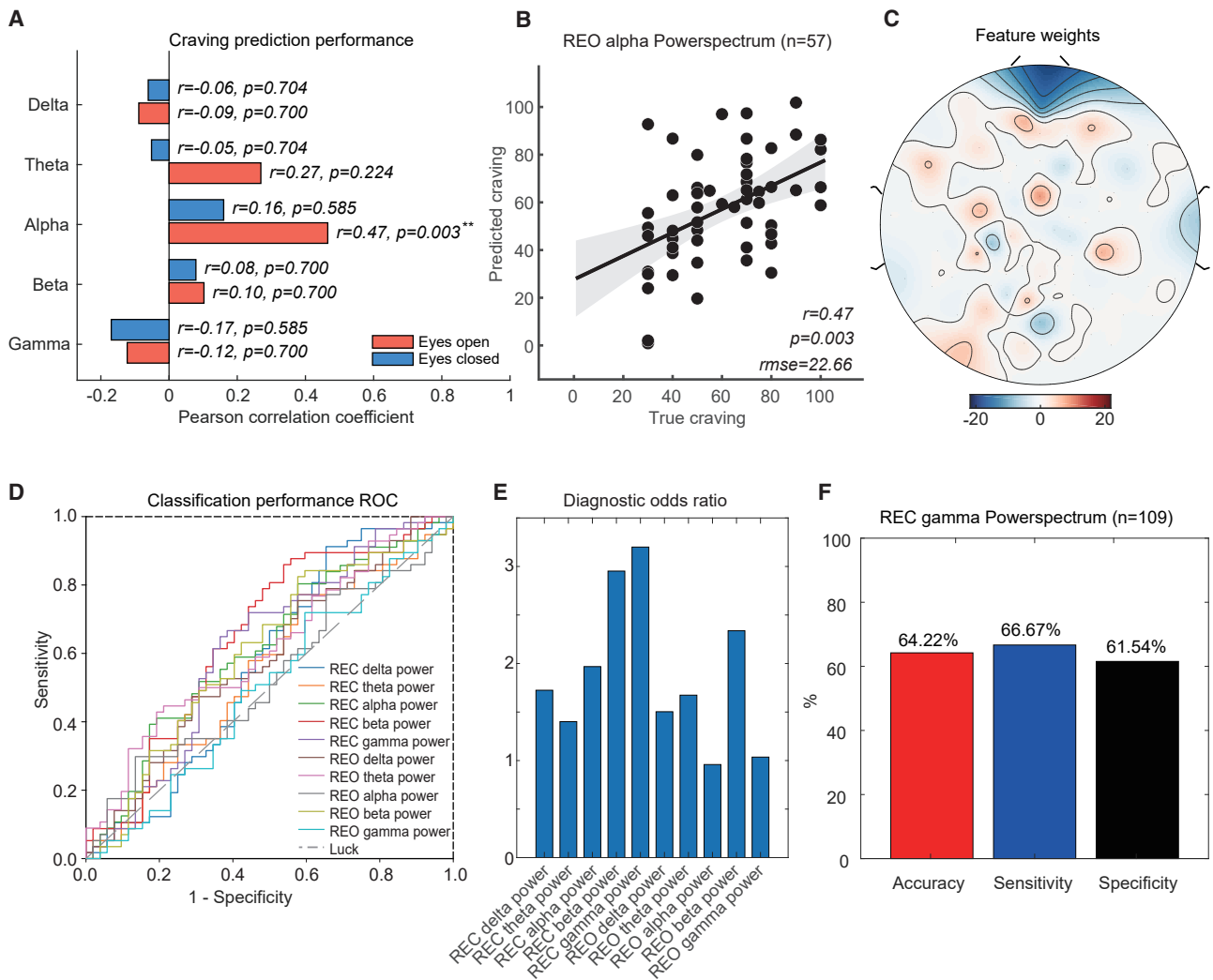
Figure 5. Craving prediction and MUD identification by sensor-space spectral power

(A) Prediction performance comparisons between different predictors. Only REO alpha power model is significantly predictive. **p < 0.01.

(B) Prediction performance using REO alpha power (Pearson's r = 0.47, p = 0.003, FDR corrected, RMSE = 22.66, n = 57 individuals with MUD). Gray: 95% confidence interval.

(C) Feature weights of REO alpha power prediction model shown in topographical plot.

(D) ROC of classification performance. The highest AUC is from the REC beta power model (AUC = 0.649).

(E) Diagnostic odds ratio of classification performance.

(F) Classification performance using REC gamma power (n = 57 individuals with MUD and 52 HC individuals). Accuracy: 64.22%, sensitivity: 66.67%, and specificity: 61.54%.

See also Figure S7.

and insula.[22] Additionally, disruptions in risk-related processing are observed in the insula of individuals with MUD.[24] A meta-analysis further indicates decreased regional metabolites in the MPFC of individuals with MUD.[25]

The correlation between the insula and the orbital gyrus in the delta band may suggest an association between the heightened awareness of bodily states and the drive for reward-seeking behaviors during craving in MUD.[26] The correlation in the beta band between LPMFG and MPFC may suggest a link between cognitive control processes and self-referential or emotional aspects of craving.[27] These specific connections could potentially serve

as targets for therapeutic interventions. Modulating the connectivity between these regions might help reduce the intensity of craving or improve cognitive control over cravings in individuals with SUD. In summary, the significant correlations between craving and these specific brain connections in the delta and beta frequency bands suggest that the interplay between regions associated with emotional processing, reward seeking, and cognitive control may be crucial for understanding the neural basis of craving in MUD. Further research is needed to fully elucidate the functional significance of these connections and their potential role in the development and treatment of addiction.

The complexity of MUD as a brain disorder has led researchers to consider neurophysiological activity as a reliable predictor of drug use and relapse.[28] Previous studies of EEG event-related potentials (ERPs) have explored their relationship with drug-seeking behaviors, but the results have been inconsistent, likely due to different responses to substance-related stimuli in different contexts.[28–30] In contrast, resting-state EEG records the spontaneous electrical activity of the brain, which is ongoing and more reliable and can be obtained more easily in clinical settings. Thus, resting-state EEG may be a more effective tool for predicting drug use and relapse in individuals with MUD and may be especially helpful for developing AI methodologies to support diagnosis of and craving prediction in MUD.

Eyes-open beta FCNs as a biomarker in craving prediction and identification of MUD

Our study sheds light on the potential of eyes-open beta FCNs as a biomarker of MUD. REO beta FCNs demonstrated predictive capabilities in evaluating cue-induced craving and correlated well with the phenomenon of craving in individuals with MUD. Although previous studies have used craving scores to predict methamphetamine use[31,32] and treatment response[33] in MUD, few have explored baseline craving evaluation through neurophysiological activities. To further understand the neurobiological biomarkers for craving in individuals with MUD, we developed a machine learning model for predicting cue-induced craving scores.

In addition to craving prediction, eyes-open beta FCNs also show potential as a biomarker for identifying abnormalities in individuals with MUD. Previous studies have investigated abnormality identification in MUD using various methods, such as arterial spin labeling,[20] EEG and galvanic skin response in drug-simulated virtual reality environments,[19] urine,[34] cue-elicited heart rate variability,[35] and weighted phase lag index.[36] Among these studies, weighted phase lag index, a type of FCN obtained from resting-state EEG at the sensor level, achieved a high classification accuracy of 93%, sensitivity of 100%, and specificity of 83%, demonstrating the potential of FCNs for classifying MUD. However, the classification model using FCNs at the sensor level failed to establish a clear relationship between brain activities and MUD. Our study, on the other hand, used source localization to obtain cortical current source density from resting-state scalp EEG, which allowed us to associate brain activities and interactions in different brain regions with MUD and establish a neurobiological biomarker pattern. To reduce the impact of volume conduction on the inverse problem, we utilized another type of FCN, iCoh.

Based on our findings, eyes-open beta FCNs appeared to be the most effective biomarker among all frequency bands and resting conditions for predicting and evaluating craving in individuals with MUD. In our previous studies, MPFC activities in the beta frequency synchronized in individuals with MUD who had been abstinent for 1–3 months.[18] Beta band oscillation has also been associated with negative symptoms in the prediction of psychosis[37,38] and has also shown good accuracy in classifying methamphetamine-dependent individuals.[36] In addition to the regions of interest (ANG (angular gyrus), INS, PCC, MFG, etc.) previously mentioned, long-term methamphetamine

exposure may lead to a reduction in cortical complexity, particularly in frontal regions,[39] as well as increased frontal delta band power in patients at clinical high risk for psychosis.[40] One study found positive connectivity between the right anterior INS and the precuneus in response to smoking cues,[41] which may be related to craving. Other studies have shown activation of MPFC neurons during cue-induced alcohol seeking in rats[42] and differences in the structure and function of brain regions related to salience evaluation (INS and ACC) in SUD.[43] Long-term-abstinent methamphetamine users have been found to exhibit decreased cortical gray matter volumes in visual associated cortices, which may contribute to psychiatric symptoms[44] and drug cue-induced craving.[45] Additionally, brain regions related to auditory/visual regulation may also play a crucial role in the psychiatric symptoms of MUD.[46,47]

The correspondence between the significant ROIs identified in our EEG functional connectivity analysis, taken together with prior research on MUD and SUDs more broadly, implies that EEG FCNs at the ROI level have the potential to act as neurobiological biomarkers for both identifying abnormalities and estimating craving in individuals with MUD.

Brain functional connectivity is a better biomarker for individuals with MUD than spectral power

Previous studies have extensively investigated the role of EEG band power in SUDs. For example, studies have shown increased alpha band power in smokers when exposed to smoking virtual reality environments,[48] altered theta band power in the medial frontal cortex (MFC) and functional connectivity between the MFC and the dorsal PFC (dPFC) in individuals with alcohol use disorder,[49] and reduced alpha band power in response to emotional and cigarette-related stimuli compared to neutral stimuli in smokers.[50] However, it is questionable whether the band power spectrum can truly reflect the neural mechanisms underlying these neurological and psychiatric disorders. A recent retrospective study on brain lesions has identified a connectomic profile including specific brain regions such as the paracingulate gyrus, the left frontal operculum, and the medial fronto-polar cortex as important in addiction remission.[51] In light of the findings in this study, lesions in specific regions or activation patterns alone may not be sufficient to interpret the neural dysfunction in individuals with MUD. Instead, changes in the activation patterns of interactions within and between specific neural circuits and systems are more likely to be associated with MUD.[52] Our findings suggest that FCNs may be better for MUD identification and craving estimation than spectral power, highlighting the need for more complex models to understand the neural mechanisms underlying MUD.

In the context of addiction, characterized by dysfunctional intercommunication among brain networks, the examination of network-level connections such as those provided by FCNs offers a comprehensive perspective on craving.[51] Craving, a multifaceted phenomenon within SUDs, involves intricate coordination across multiple brain regions.[53] FCNs emerge as invaluable tools for dissecting these complex interactions. Moreover, FCNs possess the capability to capture the temporal dynamics of connectivity patterns during craving states. Leveraging measures like iCoh, they discern authentic brain interactions from potential artifacts. Furthermore, FCN analysis unveils noteworthy

alterations in functional connectivity, a critical insight that holds particular relevance in neurological and psychiatric disorders, including SUDs.[54] These alterations in connectivity often eclipse changes in localized brain activity. This highlights the clinical promise of FCNs for advancing our comprehension and therapeutic approaches to these challenging conditions.

Conclusion

Here, we reported potential neurophysiological connectomic biomarkers for identifying abnormalities and predicting craving in MUD using resting-state high-density EEG. Our findings suggest a promising approach for clinical symptom evaluation, auxiliary diagnosis, and treatment and pave the way for oscillation-based non-invasive brain stimulation treatments for addiction.

Limitations of the study

The study has some limitations that future research should address to better understand its clinical implications. First, we did not include event-related EEG data on cue reactivity, and combining multimodal EEG data could enhance the predictive performance of the biomarkers. The procedure of cue exposure may also lead to certain network changes in the resting EEG data analyzed in the study. In future work, we are considering the inclusion of supplementary measures or scales that could provide a more comprehensive understanding of the multifaceted nature of craving in MUD. This augmentation would help enrich our data interpretation and better capture the complexity of craving experiences among our participants. Secondly, we adopted the PPC strategy measurement in the present study rather than disentangling pre-video (tonic) and cue-induced (phasic) components of craving. PPC aims to induce the most robust craving states that originate from both environmental cues and abstinence factors that also associate with several clinically significant outcomes. In the future, it is critical to carefully assess the cue-induced craving more specifically in detail and to compare the neural substrate underlying PPC and cue-induced craving. Such an adjustment will bolster the credibility of our findings and align with best practices in craving assessments. Third, high-density EEG source imaging approach may not be sensitive to subcortical neuronal activity, which can be highly relevant to communication in large-scale neural circuits. The source imaging analysis would benefit from an individualized head model with more precise anatomical information. Additionally, longitudinal and pre-post intervention EEG studies exploring biomarkers associated with abstinence/relapse or treatment are necessary before the biomarkers can be adopted clinically.

STAR★METHODS

Detailed methods are provided in the online version of this paper and include the following:

- KEY RESOURCES TABLE
- RESOURCE AVAILABILITY
  - Lead contact
  - Materials availability
  - Data and code availability
- EXPERIMENTAL MODEL AND STUDY PARTICIPANT DETAILS

- METHOD DETAILS
  - Peak provoked craving (PPC) assessment
  - EEG acquisition
  - EEG pre-processing
  - Source localization
  - Region of interest parcellation
  - Functional connectivity network calculation
  - Group level analysis
  - Machine learning analysis
  - Craving prediction in MUD individuals
  - Identification of MUD individuals
- ANALYSIS WITH SENSOR-SPACE SPECTRAL POWER
- QUANTIFICATION AND STATISTICAL ANALYSIS

AUTHOR CONTRIBUTIONS

W.T., A.E., W.W., and T.-F.Y. conceived and designed the study. W.T., D.Z., and W.W. collected the data. W.T., D.Z., J.D., S.Z., Y.Z., A.E., W.W., and T.-F.Y. analyzed the data and wrote the manuscript together.

REFERENCES

1. Paulus, M.P., and Stewart, J.L. (2020). Neurobiology, clinical presentation, and treatment of methamphetamine use disorder: A review. JAMA Psychiatr. 77, 959–966.

2. Substance Abuse and Mental Health Services Administration. (2021). National Survey of Drug Use and Health (NSDUH) Releases. https://www.samhsa.gov/data/release/2021-national-survey-drug-use-and-health-nsduh-releases.

3. Brecht, M.-L., and Herbeck, D. (2014). Time to relapse following treatment for methamphetamine use: A long-term perspective on patterns and predictors. Drug Alcohol Depend. 139, 18–25.

4. Chiang, M., Lombardi, D., Du, J., Makrum, U., Sitthichai, R., Harrington, A., Shukair, N., Zhao, M., and Fan, X. (2019). Methamphetamine-associated psychosis: Clinical presentation, biological basis, and treatment options. Hum. Psychopharmacol. 34, e2710.

5. Wise, R.A. (1988). The neurobiology of craving: Implications for the understanding and treatment of addiction. J. Abnorm. Psychol. *97*, 118–132.

6. Sayette, M.A. (2016). The role of craving in substance use disorders: Theoretical and methodological issues. Annu. Rev. Clin. Psychol. *12*, 407–433.

7. Hasin, D.S., O'Brien, C.P., Auriacombe, M., Borges, G., Bucholz, K., Budney, A., Compton, W.M., Crowley, T., Ling, W., Petry, N.M., et al. (2013). Dsm-5 criteria for substance use disorders: Recommendations and rationale. Am. J. Psychiatr. *170*, 834–851.

8. Chase, H.W., Eickhoff, S.B., Laird, A.R., and Hogarth, L. (2011). The neural basis of drug stimulus processing and craving: An activation likelihood estimation meta-analysis. Biol. Psychiatr. *70*, 785–793.

9. Childress, A.R., Hole, A.V., Ehrman, R.N., Robbins, S.J., McLellan, A.T., and O'Brien, C.P. (1993). Cue reactivity and cue reactivity interventions in drug dependence. NIDA Res. Monogr. *137*, 73–95.

10. Vafaie, N., and Kober, H. (2022). Association of drug cues and craving with drug use and relapse: A systematic review and meta-analysis. JAMA Psychiatr. *79*, 641–650.

11. Sohrabpour, A., Lu, Y., Kankirawatana, P., Blount, J., Kim, H., and He, B. (2015). Effect of eeg electrode number on epileptic source localization in pediatric patients. Clin. Neurophysiol. *126*, 472–480.

12. Michel, C.M., Lantz, G., Spinelli, L., de Peralta, R.G., Landis, T., and Seeck, M. (2004). 128-channel eeg source imaging in epilepsy: Clinical yield and localization precision. J. Clin. Neurophysiol. *21*, 71–83.

13. Sohrabpour, A., Cai, Z., Ye, S., Brinkmann, B., Worrell, G., and He, B. (2020). Noninvasive electromagnetic source imaging of spatiotemporally distributed epileptogenic brain sources. Nat. Commun. *11*, 1946.

14. Shakeshaft, A., Laiou, P., Abela, E., Stavropoulos, I., Richardson, M.P., and Pal, D.K.; BIOJUME Consortium (2022). Heterogeneity of resting-state eeg features in juvenile myoclonic epilepsy and controls. Brain Commun. *4*, fcac180.

15. Wu, W., Zhang, Y., Jiang, J., Lucas, M.V., Fonzo, G.A., Rolle, C.E., Cooper, C., Chin-Fatt, C., Krepel, N., Cornelssen, C.A., et al. (2020). An electroencephalographic signature predicts antidepressant response in major depression. Nat. Biotechnol. *38*, 439–447.

16. Pizzagalli, D.A., Webb, C.A., Dillon, D.G., Tenke, C.E., Kayser, J., Goer, F., Fava, M., McGrath, P., Weissman, M., Parsey, R., et al. (2018). Pretreatment rostral anterior cingulate cortex theta activity in relation to symptom improvement in depression: A randomized clinical trial. JAMA Psychiatr. *75*, 547–554.

17. Newton, T.F., Cook, I.A., Kalechstein, A.D., Duran, S., Monroy, F., Ling, W., and Leuchter, A.F. (2003). Quantitative eeg abnormalities in recently abstinent methamphetamine dependent individuals. Clin. Neurophysiol. *114*, 410–415.

18. Zhao, D., Zhang, M., Tian, W., Cao, X., Yin, L., Liu, Y., Xu, T.-L., Luo, W., and Yuan, T.-F. (2021). Neurophysiological correlate of incubation of craving in individuals with methamphetamine use disorder. Mol. Psychiatr. *26*, 6198–6208.

19. Ding, X., Li, Y., Li, D., Li, L., and Liu, X. (2020). Using machine-learning approach to distinguish patients with methamphetamine dependence from healthy subjects in a virtual reality environment. Brain Behav. *10*, e01814.

20. Li, Y., Cui, Z., Liao, Q., Dong, H., Zhang, J., Shen, W., and Zhou, W. (2019). Support vector machine-based multivariate pattern classification of methamphetamine dependence using arterial spin labeling. Addiction Biol. *24*, 1254–1262.

21. Nolte, G., Bai, O., Wheaton, L., Mari, Z., Vorbach, S., and Hallett, M. (2004). Identifying true brain interaction from eeg data using the imaginary part of coherency. Clin. Neurophysiol. *115*, 2292–2307.

22. Morales, A.M., Lee, B., Hellemann, G., O'Neill, J., and London, E.D. (2012). Gray-matter volume in methamphetamine dependence: Cigarette smoking and changes with abstinence from methamphetamine. Drug Alcohol Depend. *125*, 230–238.

23. Khajehpour, H., Makkiabadi, B., Ekhtiari, H., Bakht, S., Noroozi, A., and Mohagheghian, F. (2019). Disrupted resting-state brain functional network in methamphetamine abusers: A brain source space study by eeg. PLoS One *14*, e0226249.

24. Gowin, J.L., Stewart, J.L., May, A.C., Ball, T.M., Wittmann, M., Tapert, S.F., and Paulus, M.P. (2014). Altered cingulate and insular cortex activation during risk-taking in methamphetamine dependence: Losses lose impact. Addiction *109*, 237–247.

25. Smucny, J., and Maddock, R.J. (2023). Spectroscopic meta-analyses reveal novel metabolite profiles across methamphetamine and cocaine substance use disorder. Drug Alcohol Depend. *248*, 109900.

26. Su, H., Liu, Y., Yin, D., Chen, T., Li, X., Zhong, N., Jiang, H., Wang, J., Du, J., Xiao, K., et al. (2020). Neuroplastic changes in resting-state functional connectivity after rtms intervention for methamphetamine craving. Neuropharmacology *175*, 108177.

27. Zhang, R., and Volkow, N.D. (2019). Brain default-mode network dysfunction in addiction. Neuroimage *200*, 313–331.

28. Marissen, M.A.E., Franken, I.H.A., Waters, A.J., Blanken, P., Van Den Brink, W., and Hendriks, V.M. (2006). Attentional bias predicts heroin relapse following treatment. Addiction *101*, 1306–1312.

29. Parvaz, M.A., Moeller, S.J., and Goldstein, R.Z. (2016). Incubation of cue-induced craving in adults addicted to cocaine measured by electroencephalography. JAMA Psychiatr. *73*, 1127–1134.

30. Haifeng, J., Wenxu, Z., Hong, C., Chuanwei, L., Jiang, D., Haiming, S., Zhikang, C., Din, X., Jijun, W., and Min, Z. (2015). P300 event-related potential in abstinent methamphetamine-dependent patients. Physiol. Behav. *149*, 142–148.

31. Galloway, G.P., Singleton, E.G., Anglin, M.D., Rawson, R.A., Patricia, M.C., Joseph, B., Richard, B., Alison Hamilton, B., Cynthia, B., Darrell, C., et al. (2008). How long does craving predict use of methamphetamine? Assessment of use one to seven weeks after the assessment of craving. Subst Abuse. *1*, SART.S775. SART.S775.

32. Hartz, D.T., Frederick-Osborne, S.L., and Galloway, G.P. (2001). Craving predicts use during treatment for methamphetamine dependence: A prospective, repeated-measures, within-subject analysis. Drug Alcohol Depend. *63*, 269–276.

33. Yan, C., Yang, X., Yang, R., Yang, W., Luo, J., Tang, F., Huang, S., and Liu, J. (2021). Treatment response prediction and individualized identification of short-term abstinence methamphetamine dependence using brain graph metrics. Front. Psychiatr. *12*, 583950.

34. Kurnianingsih, K., Al Faridi Hadi, N.F., Dwi Wardihani, E., Kubota, N., and Chin, W.H. (2020). Ensemble learning based on soft voting for detecting methamphetamine in urine. In 2020 IEEE International Conference on Fuzzy Systems (FUZZ-IEEE).

35. Wang, Y.-G., Shen, Z.-H., and Wu, X.-C. (2018). Detection of patients with methamphetamine dependence with cue-elicited heart rate variability in a virtual social environment. Psychiatr. Res. *270*, 382–388.

36. Khajehpour, H., Mohagheghian, F., Ekhtiari, H., Makkiabadi, B., Jafari, A.H., Eqlimi, E., and Harirchian, M.H. (2019). Computer-aided classifying and characterizing of methamphetamine use disorder using resting-state eeg. Cogn. Neurodyn. *13*, 519–530.

37. Zimmermann, R., Gschwandtner, U., Wilhelm, F.H., Pflueger, M.O., Riecher-Rössler, A., and Fuhr, P. (2010). Eeg spectral power and negative symptoms in at-risk individuals predict transition to psychosis. Schizophr. Res. *123*, 208–216.

38. Gschwandtner, U., Zimmermann, R., Pflueger, M.O., Riecher-Rössler, A., and Fuhr, P. (2009). Negative symptoms in neuroleptic-naïve patients with first-episode psychosis correlate with qeeg parameters. Schizophr. Res. *115*, 231–236.

39. Kim, S.J., Lyoo, I.K., Hwang, J., Sung, Y.H., Lee, H.Y., Lee, D.S., Jeong, D.-U., and Renshaw, P.F. (2005). Frontal glucose hypometabolism in abstinent methamphetamine users. Neuropsychopharmacol *30*, 1383–1391.

40. van Tricht, M.J., Ruhrmann, S., Arns, M., Müller, R., Bodatsch, M., Velthorst, E., Koelman, J.H.T.M., Bour, L.J., Zurek, K., Schultze-Lutter, F., et al. (2014). Can quantitative eeg measures predict clinical outcome in subjects at clinical high risk for psychosis? A prospective multicenter study. Schizophr. Res. *153*, 42–47.

41. Moran-Santa Maria, M.M., Hartwell, K.J., Hanlon, C.A., Canterberry, M., Lematty, T., Owens, M., Brady, K.T., and George, M.S. (2015). Right anterior insula connectivity is important for cue-induced craving in nicotine-dependent smokers. Addiction Biol. *20*, 407–414.

42. Pfarr, S., Meinhardt, M.W., Klee, M.L., Hansson, A.C., Vengeliene, V., Schönig, K., Bartsch, D., Hope, B.T., Spanagel, R., and Sommer, W.H. (2015). Losing control: Excessive alcohol seeking after selective inactivation of cue-responsive neurons in the infralimbic cortex. J. Neurosci. *35*, 10750–10761.

43. Tanabe, J., Regner, M., Sakai, J., Martinez, D., and Gowin, J. (2019). Neuroimaging reward, craving, learning, and cognitive control in substance use disorders: Review and implications for treatment. Br. J. Radiol. *92*, 20180942.

44. Nakama, H., Chang, L., Fein, G., Shimotsu, R., Jiang, C.S., and Ernst, T. (2011). Methamphetamine users show greater than normal age-related cortical gray matter loss. Addiction *106*, 1474–1483.

45. Zhang, Z., He, L., Huang, S., Fan, L., Li, Y., Li, P., Zhang, J., Liu, J., and Yang, R. (2018). Alteration of brain structure with long-term abstinence of methamphetamine by voxel-based morphometry. Front. Psychiatr. *9*, 722.

46. Liu, Y., Li, Q., Zhang, T., Wang, L., Wang, Y., Chen, J., Zhu, J., Shi, H., Wang, W., and Li, W. (2022). Differences in small-world networks between methamphetamine and heroin use disorder patients and their relationship with psychiatric symptoms. Brain Imaging Behav. *16*, 1973–1982.

47. Van Hedger, K., Keedy, S.K., Schertz, K.E., Berman, M.G., and de Wit, H. (2019). Effects of methamphetamine on neural responses to visual stimuli. Psychopharmacol. *236*, 1741–1748.

48. Tamburin, S., Dal Lago, D., Armani, F., Turatti, M., Saccà, R., Campagnari, S., and Chiamulera, C. (2021). Smoking-related cue reactivity in a virtual reality setting: Association between craving and eeg measures. Psychopharmacol. *238*, 1363–1371.

49. Harper, J., Malone, S.M., and Iacono, W.G. (2017). Testing the effects of adolescent alcohol use on adult conflict-related theta dynamics. Clin. Neurophysiol. *128*, 2358–2368.

50. Cui, Y., Versace, F., Engelmann, J.M., Minnix, J.A., Robinson, J.D., Lam, C.Y., Karam-Hage, M., Brown, V.L., Wetter, D.W., Dani, J.A., et al. (2013). Alpha oscillations in response to affective and cigarette-related stimuli in smokers. Nicotine Tob. Res. *15*, 917–924.

51. Joutsa, J., Moussawi, K., Siddiqi, S.H., Abdolahi, A., Drew, W., Cohen, A.L., Ross, T.J., Deshpande, H.U., Wang, H.Z., Bruss, J., et al. (2022). Brain lesions disrupting addiction map to a common human brain circuit. Nat. Med. *28*, 1249–1255.

52. Fedota, J.R., and Stein, E.A. (2015). Resting-state functional connectivity and nicotine addiction: Prospects for biomarker development. Ann. N. Y. Acad. Sci. *1349*, 64–82.

53. Kronberg, G., and Goldstein, R.Z. (2023). An fmri marker of drug and food craving. Nat. Neurosci. *26*, 178–180.

54. Sha, Z., Wager, T.D., Mechelli, A., and He, Y. (2019). Common dysfunction of large-scale neurocognitive networks across psychiatric disorders. Biol. Psychiatr. *85*, 379–388.

55. Wu, W., Keller, C.J., Rogasch, N.C., Longwell, P., Shpigel, E., Rolle, C.E., and Etkin, A. (2018). Artist: A fully automated artifact rejection algorithm for single-pulse tms-eeg data. Hum. Brain Mapp. *39*, 1607–1625.

56. Tipping, M.E. (2001). Sparse bayesian learning and the relevance vector machine. J. Mach. Learn. Res. *1*, 211–244.

57. Delorme, A., and Makeig, S. (2004). Eeglab: An open source toolbox for analysis of single-trial eeg dynamics including independent component analysis. J. Neurosci. Methods *134*, 9–21.

58. Bell, A.J., and Sejnowski, T.J. (1995). An information-maximization approach to blind separation and blind deconvolution. Neural Comput. *7*, 1129–1159.

59. Tadel, F., Baillet, S., Mosher, J.C., Pantazis, D., and Leahy, R.M. (2011). Brainstorm: A user-friendly application for meg/eeg analysis. Comput. Intell. Neurosci. *2011*, 879716.

60. Gramfort, A., Papadopoulo, T., Olivi, E., and Clerc, M. (2010). Openmeeg: Opensource software for quasistatic bioelectromagnetics. Biomed. Eng. Online *9*, 45.

61. Sridharan, D., Levitin, D.J., and Menon, V. (2008). A critical role for the right fronto-insular cortex in switching between central-executive and default-mode networks. Proc. Natl. Acad. Sci. USA *105*, 12569–12574.

62. Chen, A.C., Oathes, D.J., Chang, C., Bradley, T., Zhou, Z.-W., Williams, L.M., Glover, G.H., Deisseroth, K., and Etkin, A. (2013). Causal interactions between fronto-parietal central executive and default-mode networks in humans. Proc. Natl. Acad. Sci. USA *110*, 19944–19949.

63. Rubega, M., Carboni, M., Seeber, M., Pascucci, D., Tourbier, S., Toscano, G., Van Mierlo, P., Hagmann, P., Plomp, G., Vulliemoz, S., and Michel, C.M. (2019). Estimating eeg source dipole orientation based on singular-value decomposition for connectivity analysis. Brain Topogr. *32*, 704–719.

64. Oostenveld, R., Fries, P., Maris, E., and Schoffelen, J.-M. (2011). Fieldtrip: Open source software for advanced analysis of meg, eeg, and invasive electrophysiological data. Comput. Intell. Neurosci. *2011*, 156869.

65. Glas, A.S., Lijmer, J.G., Prins, M.H., Bonsel, G.J., and Bossuyt, P.M.M. (2003). The diagnostic odds ratio: A single indicator of test performance. J. Clin. Epidemiol. *56*, 1129–1135.

STAR★METHODS

KEY RESOURCES TABLE

REAGENT or RESOURCE	SOURCE	IDENTIFIER
Software and algorithms		
MATLAB 2021a	MATLAB	N/A
PyCharm 2019.3	Python	N/A
MATLAB package: ARTIST	Wu et al.[55]	https://www.altoneuroscience.com/artist
MATLAB package: EEGLAB 14.1.1	EEGLAB	https://sccn.ucsd.edu/eeglab/index.php
MATLAB package: Fieldtrip version 20180221	Fieldtrip Toolbox	https://www.fieldtriptoolbox.org
MATLAB package: BrainStorm 3.210507	BrainStorm	https://neuroimage.usc.edu/brainstorm/Introduction
MATLAB package: BrainNet Viewer 1.63	BrainNet Viewer	https://www.nitrc.org/projects/bnv/
MATLAB package: Relevance vector machine	Tipping et al.[56]	https://github.com/iqiukp/RVM-MATLAB
Python package: scikit-learn 0.24.1	scikit-learn	https://scikit-learn.org/stable/
Circos 0.69	Circos	http://circos.ca/software/download/circos/

RESOURCE AVAILABILITY

Lead contact
Further information and requests for resources should be directed to and will be fulfilled by the lead contact, Ti-Fei Yuan (ytf0707@126.com).

Materials availability
This study did not generate new unique reagents.

Data and code availability
- All original data reported in this paper will be shared by the lead contact upon request.
- All data analysis and visualization in this study are implemented based on Python 3.7 and MATLAB 2021a. Custom codes used in this study are available in the GitHub repository at https://github.com/Weiwen-Tian/EEG_MUD/tree/main and are publicly available as of the date of publication.
- Any additional information required to reanalyze the data reported in this paper is available from the lead contact upon request.

EXPERIMENTAL MODEL AND STUDY PARTICIPANT DETAILS

A total of 162 male individuals with MUD aged between 21 and 54 years old were recruited from four drug addiction rehabilitation centers (Tiantanghe, Dalianshan, Taihu and Wuhan). Inclusion criteria included: (1) Subjects whose diagnosis was MUD for more than two years, using more than 0.1 g per day on average, and reported urine drug screening test positive for methamphetamine before entering rehabilitation centers; (2) Subjects who met diagnostic criteria for MUD according to the fifth edition of the American Psychiatric Association's Diagnostic and Statistical Manual of Mental Disorder (DSM-5); (3) Subjects who didn't have other substances use disorders, including heroin, marijuana, methcathinone, alcohol, etc., as their primary addiction diagnosis in the most recent five years. An experienced psychiatrist confirmed the diagnosis of MUD. A total of 68 healthy subjects were also recruited as controls, and the two groups were matched for age, education, smoking, and drinking status. Exclusion criteria were current or historical neurological, psychiatric, or medical disorders and the use of any medication within the past three months. See Figure S1 for further details.

At the rehabilitation centers, all individuals with MUD received standardized rehabilitation procedures, including daily physical exercise and supportive therapy for relapse prevention. These participants maintained abstinence throughout the study. Ethics approval was granted by the Research Ethics Boards of Shanghai Mental Health Center and the four rehabilitation centers. All participants were well-informed and provided written informed consent in accordance with the Declaration of Helsinki. They were also compensated for their time.

Peak provoked craving (PPC) assessment and resting-state Electroencephalography (EEG) were conducted. The study also included behavioral measurements, such as the Pittsburgh Sleep Quality Index (PSQI), Beck Depression Inventory (BDI-II), Barratt Impulsivity Scale (BIS-II) sub-scores (attention, motor, no plan, and total impulsiveness), and Barratt Anxiety Inventory (BAI).

METHOD DETAILS

Peak provoked craving (PPC) assessment

To assess peak provoked craving (PPC) or maximal craving status, participants were exposed to a 5-min video presentation that vividly depicted scenarios involving methamphetamine use. This video presentation was thoughtfully designed to engage participants and evoke reactions that mirror real-world situations. After viewing the video, participants engaged in a critical aspect of our evaluation – the completion of a visual analogue scale (VAS). On this scale, participants were prompted to express their subjective experience of craving by assigning a value along a continuum. Ranging from 0 (indicating a complete absence of desire) to 100 (representing an intense and overwhelming urge), the VAS enabled participants to articulate their craving level with precision.

EEG acquisition

EEG data were acquired with a high-density, 128-electrode array (Electrical Geodesics, Inc.) using high-impedance amplifiers. All scalp channels were adjusted to maintain an impedance of <50 kΩ. The sampling rate was 500 Hz, and offline filtering was performed with a bandpass filter of 0.01–100Hz (with a notch filter at 50Hz). Participants were instructed to remain awake and relaxed while sitting in a quiet room for 5 min with eyes closed, followed by 5 min of fixating on a given point with their eyes open, and another 5 min with their eyes closed (some participants completed an additional 5 min of eyes-open recording). Custom MATLAB scripts were used for preprocessing and source localization. The resting-state eyes-closed condition yielded a total of 604.7 ± 57.3 s of EEG recordings, while the resting-state eyes-open condition yielded 268.0 ± 69.4 s of EEG recordings (mean ± std).

After ensuring demographic information (age and education years) matched and excluding subjects who did not pass strict pre-processing quality control, we included 57 MUD subjects from dataset 1, 44 MUD subjects from dataset 2, and 52 HC subjects in our study. Dataset 1 and dataset 2 were recruited independently with different individuals. Please refer to Table 1 for detailed demographic and clinical characteristics, and to Figure S1 for a flowchart illustrating the procedure.

EEG pre-processing

Offline preprocessing of EEG recordings was conducted with the EEGLAB toolbox[57] in MATLAB.

In general, the preprocessing process was as follows: first, the time series was down-sampled to 250Hz, with notch filtering to remove 50 Hz power frequency noise and bandpass filtering between 1 Hz and 100 Hz by a zero-phase finite impulse response filter. Then bad channels including bridged channels and noise channels were removed and spherically interpolated. Paroxysmal segments were rejected and excised. To remove artifacts such as blinks, eye movements, heartbeat and myoelectricity, independent components analysis (ICA) with the extend information maximization algorithm[58] was used to decompose independent components. Then bad components were detected and removed by principal components analysis (PCA) through dimensionality reduction and the least number of principal components which accounted for more than 99.9% of the total variance was determined as the number of dimensions. After the last re-reference, preprocessed EEG time series were obtained. With custom pipelines and EEG expert validation, extremes of flatline amplitudes or aberrant points, channel correlations and robust paroxysmal spike measures could be detected and removed by an automated algorithm.[55] Preprocessed time series at the sensor level were filtered into 5 canonical frequency bands: delta (1–3 Hz), theta (4–7 Hz), alpha (8–12 Hz), beta (13–30 Hz) and gamma (31–50 Hz).

Source localization

Source localization was performed using the standard head model in the Brainstorm toolbox.[59] A three-layer symmetric boundary element model of the head was computed with OpenMEEG[60] and then rotating dipoles of 3003 vertices on the cortical surface were selected. We estimated the imaging kernel, which mapped from the sensor-level EEG to the source-level current source density, using the minimum norm estimation approach (MNE) with depth weighting and regularization. Subsequently, we reduced the current density time series in three space dimensions for each vertex to one dimension from three orthogonal axes by PCA.

Region of interest parcellation

Connectivity analysis was performed among 31 ROIs in the Montreal Neurological Institute (MNI) space, derived from an independent parcellation of resting-state fMRI functional connectivity based on the peaks of the ICA clusters.[61,62] Time series representing the main pattern of variation of all vertices in the same ROI were generated through PCA. We extracted the dominant signal of the time series using singular-value decomposition (SVD), considering the first singular vector as the signal at the ROI level.[63]

These 31 ROIs were divided into 6 networks: VIS (Visual Network): Visual Area 1 (V1); SMN (Somatosensory Network): Somatosensory Cortex (SMC); DAN (Dorsal Attention Network): Inferior Frontal Junction (IFJ), Intraparietal Sulcus (IPS), Frontal Eye Fields (FEF) and Supplementary Eye Fields (SEF); DMN (Default Mode Network): Posterior Cingulate Cortex (PCC), Medial Prefrontal Cortex (MPFC) and Angular Gyrus (ANG); FPN (Frontoparietal Control Network): Posterior Middle Frontal Gyrus (PMFG), Inferior Parietal

Lobule (IPL), Orbital Gyrus (ORB) and Middle Temporal Gyrus (MTG); and VAN (Ventral Attention Network): Anterior Middle Frontal Gyrus (AMFG), Insula (INS), Dorsal Anterior Cingulate Cortex (DACC) and Supramarginal Gyrus (SUP).

Functional connectivity network calculation

Functional Connectivity Networks (FCNs) play a crucial role in capturing dynamic interactions by examining the temporal correlations or phase synchronization among multiple brain regions. Coherency and coherence are two widely used methods for analyzing EEG connectivity. To reduce the influence of volume conduction, a solution was developed that involves extracting the imaginary coherence, which represents the time delay between two channels.[21] In this study, we used imaginary coherence (iCoh) to reveal cortical interactions. Here the Fieldtrip toolbox was used to compute the iCoh connectivity of 465 unique ROI pairs in each of the 5 carrier bands and each of the 2 resting eye conditions.[64]

Denoting $S_{ij,t}$ as the cross-spectral density of $x_i(t)$ and $x_j(t)$ at time point or trial t, $S_{ij,t}$ is defined as

$$S_{ij,t}(f) = \;<x_{i,t}(f)x_{j,t}{}^*(f)> ,$$

where * means complex conjugation and $<\;>$ means expectation value.

Denoting $S_{ij}(f)$ as the cross-spectrum, the imaginary coherence is defined as

$$iCoh_{ij}(f) \;=\; Imag(Coh_{ij}(f)) \;=\; \frac{Imag(S_{ij}(f))}{\sqrt{S_{ii}(f)\cdot S_{jj}(f)}},$$

where $Coh_{ij}(f)$ is the complex form of coherency.

Calculating this connectivity at the ROI level by averaging correlations of each source-space vertex between two given ROI nodes could lead to errors due to the anti-symmetry of the imaginary part ($iCoh_{ij}(f) = \; -iCoh_{ji}(f)$). Therefore, to avoid such errors, we directly calculated the iCoh at the ROI level in the carrier frequency bands.

Group level analysis

We first performed a group-level analysis of the source-space FCNs. To investigate the relationship between craving and FCNs, we computed the correlations between these two factors while correcting the p values for multiple comparisons using false discovery rate (FDR) adjustment. Additionally, we conducted an independent t-test to compare FCNs between individuals with MUD and healthy controls (HCs), with p values for each pair of functional connectivity corrected using FDR adjustment. Furthermore, we calculated the correlations between craving and behavioral measurements while correcting with FDR adjustment.

Machine learning analysis

We used two machine learning models, based on two biomarkers (craving prediction and abnormality identification), to evaluate the strength of the relationship. For both models, each ROI pair connectivity measure was used. See Figure 1 for an illustration of our data processing framework, and Figure S2 for the machine learning workflow.

Cross validation: The data were randomly divided into 10 subsets, with each subset containing approximately the same number of subjects. One subset was selected as the test data and the other 9 subsets were used as training data. This process was repeated 10 times, with each of the 10 subsets used once as the test data. As a result, each subject had a predicted probability. To improve the stability of the prediction, the data were randomized 10 times, and the stratified 10-fold cross-validation was run on each randomized set of data. Details of the cross-validation are illustrated in Figure S2A.

Machine learning workflow: Outlier data, defined as having a sum of feature values more than three median absolute deviations (MAD) from the median, were removed from the EEG connectivity feature vectors. The dataset was then *Z* score normalized, and the processed EEG FCNs were used as input features for the machine learning models. For predicting craving scores, the RVM model and 10*10 cross-validation were applied to the dataset for predicting craving scores and classifying individuals with MUD and HCs. Pearson's correlation coefficient (r) and root-mean-square error were calculated to evaluate the prediction model, while accuracy, sensitivity, specificity, diagnostic odds ratio, and area under the ROC curve were calculated to evaluate the classification model. The machine learning workflow is illustrated in Figure S2B.

Relevance vector machine: A relevance vector machine (RVM) with the linear kernel of EEG data was used to build sparse linear regression models for craving prediction from connectivity features.[56] We also employed an RVM with the linear kernel of EEG data and an outer layer of a sigmoid function to build sparse classification models to distinguish MUD and HCs. An RVM is a machine learning technique that automatically selects relevant features for prediction by maximizing the marginal likelihood with a sparse prior to penalize complex models under the sparse Bayesian learning framework. Compared to a support vector machine (SVM), an RVM can provide probabilistic predictions, reduce computational complexity, and estimate the error/margin trade-off parameter. Additionally, the kernel function of an RVM does not need to satisfy Mercer's condition, which means it works without additional validation to determine the hyperparameters.[56]

Craving prediction in MUD individuals

We used the RVM model with 10-time 10-fold cross-validation to predict craving scores in individuals with MUD based on resting FCNs among the ROIs. We assessed the predictive performance by calculating Pearson's correlation coefficient and root-mean-

square error (RMSE) between the cross-validated predicted scores and true scores. We also reported the p values, after correction for multiple comparisons using the FDR method, for the one-tailed alternative hypothesis that the coefficient of determination was greater than 0 for iCoh of 5 bands in resting eyes-open and eyes-closed conditions (a total of 10 patterns). Additionally, since the RVM model was a sparse model, we used the feature weight matrix of the RVM model to indicate the predictive importance and ability of brain functional connections.

Identification of MUD individuals

The RVM model with 10-time 10-fold cross-validation was used to classify individuals with MUD and HCs based on EEG functional connectivity estimates. The model assigned a label of '1' to individuals with MUD and '0' to HCs. Classification performance was assessed using classification accuracy, sensitivity (true positive rate), specificity (true negative rate), and area under the receiver operating characteristic curve (AUC). AUC was calculated by scikit-learn package in python (https://scikit-learn.org/stable/). AUC represents the resolution of the model in distinguishing between different categories. It measures the ability of the model to correctly discriminate between positive and negative instances, indicating how well the model separates the classes based on the chosen evaluation criteria. Higher AUC values indicated better separability and higher classification performance. The diagnostic odds ratio, defined as the ratio of the odds of a positive test when the subject has a disease to the odds of a positive test when the subject does not have the disease,[65] was also calculated to measure the effectiveness of our classification model.

ANALYSIS WITH SENSOR-SPACE SPECTRAL POWER

To test the predictive ability of FCNs in individuals with MUD, we also used sensor-space power spectra as input features for the machine learning models and compared the classification and predictive performance between FCNs and band power spectra.

QUANTIFICATION AND STATISTICAL ANALYSIS

Statistical analysis was performed by Excel and MATLAB. The statistical details of experiments can be found in the figure legends. Significant difference between two groups was evaluated by two-sided Student's t test. Correlation between two variables was evaluated by Pearson's correlation coefficient. Correction for multiple comparisons with false discovery rate (FDR) method was conducted. $p < 0.05$ was considered as statistically significant. *, **, and *** indicate statistical significance at $p < 0.05$, $p < 0.01$, and $p < 0.001$, respectively.